NACA

RESEARCH MEMORANDUM

AN ASSESSMENT OF THE AIRPLANE DRAG PROBLEM AT TRANSONIC AND SUPERSONIC SPEEDS

By Charles J. Donlan

Langley Aeronautical Laboratory
Langley Field, Va.

NATIONAL ADVISORY COMMITTEE
FOR AERONAUTICS

WASHINGTON
July 15, 1954

NACA RM L54F16

NATIONAL ADVISORY COMMITTEE FOR AERONAUTICS

RESEARCH MEMORANDUM

AN ASSESSMENT OF THE AIRPLANE DRAG PROBLEM AT TRANSONIC AND SUPERSONIC SPEEDS[1]

By Charles J. Donlan

SUMMARY

The airplane drag problem at transonic and supersonic speeds is discussed. The area rule is shown to be a powerful tool that provides guidance for the airplane designer in selecting aerodynamic features compatible with low wave drag. The factors influencing the drag of bodies of revolution are reviewed and the effectiveness in reducing wave drag of various methods of improving the cross-sectional area distribution of aircraft configurations is illustrated. It is demonstrated that, irrespective of the method adopted for improving area distribution, a high effective fineness ratio and smooth area progressions along the equivalent body are essential to the achievement of low drag.

INTRODUCTION

The airplane designer is interested in achieving the lowest possible drag for his configuration. For aircraft that fly at less than the speed of sound, this requires the minimization of the profile drag - essentially friction drag - and the induced drag. For aircraft that are to fly at transonic and supersonic speeds, another source of drag must be considered - the wave-making drag. The drag from this source alone can create formidable design problems as illustrated in figure 1. For the flight condition assumed, the drag coefficient associated with level flight increases markedly with Mach number as the speed of sound is approached and exceeded. It is evident that, while the friction-drag component and the trim-drag component (including induced drag) are still of significance at supersonic speeds, the wave-drag component is responsible for the large increase in drag coefficient shown. The wave-drag component is primarily independent of the lift and thus can usually be analyzed for the zero-lift condition (C_{D_0}). Because it is of such great

[1]This paper was originally prepared as an informal talk and was presented at a meeting of the NACA Committee on Aerodynamics held at the Langley Aeronautical Laboratory on April 28, 1954.

importance in establishing the level of the drag curve, a large research effort has been devoted toward methods of reducing this source of drag. This paper, therefore, is concerned primarily with the progress that has been made in coping with the wave-drag problem.

SYMBOLS

A	cross-sectional area of body; also, aspect ratio
b	wing span
C_D	drag coefficient
$C_{D_{min}}$	minimum drag coefficient
C_{D_o}	zero-lift drag coefficient
$\Delta C_{D_{CALC}}$	calculated drag-rise coefficient
$\Delta C_{D_{EQ.B}}$	drag-rise coefficient of equivalent body
$\Delta C_{D_{EXP}}$	experimental drag-rise coefficient
$\left(\Delta C_D\right)_F$	drag-rise coefficient based on frontal area
$\Delta C_{D_{WB}}$	drag-rise coefficient of wing-body configuration
C_T	thrust coefficient
c	airfoil chord
d_{max}	maximum body diameter
l	body length
M	Mach number
t	airfoil thickness
Λ_{LE}	leading-edge sweep

[redacted]

λ taper ratio

X distance from nose of body

THE AREA RULE

The key to understanding why certain arrangements of airplane components result in less wave drag at transonic speeds than others is furnished by the aerodynamic principles expressed so conveniently in the so-called area rule. These important aerodynamic principles were demonstrated experimentally less than two years ago by Whitcomb (ref. 1) and the effect on airplane design philosophy has been noteworthy. In this brief period of time nearly every transonic and supersonic airplane design has been influenced in some way by area-rule concepts. The reason for its acceptance is that the area rule provides the airplane designer with a tool that permits him to assess those features of a design that should be sought for - or avoided - if wave drag is to be kept to a minimum.

The equivalent-body concept.- Figure 2 illustrates the basic tenet of the area rule, which states that the wave drag of an airplane configuration depends primarily on the longitudinal distribution of the total cross-sectional area. This concept results in the proposition that the wave drag of a simple equivalent body of revolution (that is, a body having the same longitudinal distribution of total cross-sectional area) would be the same as the drag of the more complex wing-body arrangement. The cross-sectional distributions shown are obtained by passing planes perpendicular to the body axis. This procedure is correct for a design Mach number of 1.0. Although originally developed as a Mach number 1.0 concept, the area rule has been extended to supersonic speeds by Whitcomb (ref. 2) and R. T. Jones (ref. 3), who has elegantly molded this concept into the framework of linearized body theory. In the supersonic applications of the area rule, the geometric considerations involve the cross-sectional distributions formed by planes tangent to the Mach cone at various orientations about the longitudinal axis of the configuration.

Experimental verification.- The equivalent-body concept has been subjected to experimental verification. In figure 3 (from ref. 4), the measured drag-rise increments at $M = 1.03$ for various swept-wing, delta-wing, and unswept-wing—body combinations and complete airplanes (all symbolized by $\Delta C_{D_{WB}}$) are compared with the experimental increments for the equivalent bodies of revolution $\left(\Delta C_{D_{EQ.B}}\right)$. The aspect ratios of the wings are 4 or less and the wing thickness-chord ratios (streamwise) are 0.07 or less. Deviations from exact agreement are apparent but, in general, qualitative agreement exists between the drag-rise increments, and thus the basic tenet of the area rule appears to be substantiated.

[redacted]

Progress in calculations.- Utilizing the linear-theory development of Jones (ref. 3), Holdaway (ref. 5) has computed the drag rise of several wing-body-tail configurations at various Mach numbers and compared his results with the experimental drag-rise values obtained with freely falling models. This comparison is presented in figure 4. The agreement is good in the regions where the drag rise is lowest, although precise determination of drag - for example, $\Delta C_D \lesssim 0.0015$ - should not be expected from any computation based on an approximate theory. It is significant, however, that the calculated results appear to be as reliable for drag predictions near $M = 1$ as actual experiments with equivalent bodies (fig. 3), and for supersonic applications the theoretical procedure is to be preferred. The theoretical method outlined in reference 5 is perhaps the only published procedure available that will handle transonic and supersonic calculations of this nature in a relatively routine manner. Nelson and Stoney (ref. 6) have published an empirical correlation of drag-rise data that permits estimates of drag-rise increments around $M = 1$ but the method has not been extended to supersonic speeds.

BODY DRAG

Knowing that the transonic drag rise of his airplane will reflect the merits of its equivalent body, it is obvious that the airplane designer would want his design to have a low-drag equivalent body shape. Figure 5 shows some of the factors governing the drag of bodies at transonic and supersonic speeds and illustrates the penalties imposed by low fineness ratios and deviations from low-drag shapes. The drag-rise coefficient $(\Delta C_D)_F$ in this figure is based on body frontal area. The points represent all types of smooth parabolic bodies for which rocket-model drag data are available. The lowest drags are obtained with bodies possessing smooth parabolic profiles. The minimum drag variation will be found to be inversely proportional to the square of the fineness ratio, as theory predicts. For a given fineness ratio ($l/d_{max} = 9$, for example), the bodies well removed from the minimum drag curve are found to possess steep gradients in their area distributions, as shown. It is clear that the requirement for low drag is a high effective fineness ratio and a smooth area distribution free of rapid rates of change of area along the body. The position of the maximum diameter for minimum drag is a function of the base area and for bodies pointed on either end it is at $0.5l$. One could substitute a Sears-Haack shape or some other profile for the parabolic shape used here with similar results. At the higher fineness ratios that are required for really low drag, however, the particular choice of body shape is a minor variable as far as drag is concerned.

[redacted]

AIRPLANE DRAG

Figure 6 is prepared in the same fashion as figure 5 except that the points are for complete airplane configurations. The drag-rise coefficient $(\Delta C_D)_F$ again is based on the frontal area and overall fineness ratio of the equivalent bodies of revolution. The minimum measured body-drag curve and the theoretical variation are replotted from figure 5. The open points represent the drag of basic or initial configurations. The closed and half-closed points are experimental results obtained with modifications that were made to the basic configuration in order to improve the effective fineness ratio of the equivalent body. These modifications were of several kinds. It is of interest to examine a few of the cases shown to highlight some of the experiences of the NACA in utilizing various methods such as body indentation, body lengthening, body buildup, and the juggling of the aircraft components themselves in order to approach the high-fineness-ratio smooth equivalent body for which there is no substitute if low drag is to be achieved.

Example A.- A partial case history of a delta-wing model identified as example A is summarized in figure 7. The composition of the area diagram of the prototype configuration is shown in the upper left-hand portion of the figure. Note how each element piles on top of the other, especially at the rear of the fuselage. The rate of change of area with length at the rear of the fuselage is thus very rapid and the large suction forces associated with this area gradient at transonic speeds is responsible for the high drag rise of the prototype configuration. In the lower right of the figure, the area distribution of the prototype is compared with the area distribution of the modification. By "waisting" or indenting the body to accommodate the wing, partially, and by lengthening the fuselage, the area distribution of the revised configuration is obviously improved and this improvement is reflected in the lower drag levels for the revised design. Even larger reductions in drag are possible if, in addition to the modifications incorporated in the revised design, the nose of the aircraft could be changed in the region shown in the area diagram.

In order to show what these drag gains mean in airplane performance, the drag in pounds has been evaluated for a selected flight condition and compared with the available thrust in figure 8. It will be seen that, while the prototype will just about attain sonic speed in level flight, the revised airplane could fly level at $M = 1.15$. More startling performance gains are possible with the improved nose configuration.

Example B.- Figure 9 illustrates how adding volume to an unswept-wing configuration (example B) so as to improve the area distribution can result in a lower drag configuration. The left plot of the figure

[redacted]

illustrates the M = 1 modification that is example B on figure 6. The right portion of the figure illustrates a supersonic application at M = 1.14. The experiments were conducted with free-fall models and the calculations were carried out by Holdaway by use of the procedures in reference 5. The volume is added in such a manner that a Sears-Haack minimum-drag shape is created although for the M = 1.14 case, such a shape must necessarily represent only an average distribution. The dashed curve represents the drag of the original configuration. The points are for the modified configuration. The solid lines are from theoretical calculations. The drag improvements are significant and the agreement between the experiments and the calculations remarkable.

Example C.- In figure 10 is shown an example of how adding volume rearward of the maximum cross section of a swept-wing airplane (example C) reduced the severe area gradient and thus significantly reduced the drag rise. The volume is added fairly symmetrically around the fuselage. Eighty percent of the inlet-stream-tube area was allowed for in preparing the area diagram. The wing-root inlet location precluded any improvement in the area diagram ahead of the wing in this case.

It is of interest that, in this case, the transonic drag was reduced by virtue of an improvement in the afterbody area distribution despite the fact that the maximum cross-sectional area was actually increased somewhat. Although not shown in this figure, some reduction in the drag level has been found to be still evident at a Mach number of 2.0, not withstanding that the modification was laid out for a Mach number of 1.0.

Example D.- Thus far, the examples have all been of configurations characterized by engines installed in the fuselage. An interesting example of the application of area-rule principles to a configuration with nacelles (example D) is summarized in figure 11. The undesirable superposition of components on the original arrangement is evident from the area diagram on the left-hand plot of the figure. The modified design at the right uses elements in themselves of high fineness ratio and so positioned that the resulting area distribution approaches a parabola over much of its length. Although the area distribution was laid out for M = 1, the components are all of such excellent proportion in themselves and the contouring is accomplished over such long lengths and with such gentle slopes that the distribution apparently remains good even for supersonic speeds up to M = 1.4, as the drag results indicate. Even in this case, however, the irregularities in the area distribution are costly and the drag of the equivalent body is actually considerably higher than that of a true parabolic body of equal fineness ratio, as can be seen from figure 6.

It is not always possible to use a completely symmetrical arrangement such as was used here and items such as off-center position of the wing, incidence of the wing, and noncircular cross sections constitute items for continued research.

[redacted]

LOW-DRAG ARRANGEMENTS

In the examples cited, the effectiveness of certain kinds of modifications in reducing the zero-lift drag has been illustrated. Such applications have not been 100 percent successful and continued research is needed to determine how the drag of such configurations can be made to approach more nearly that which might be expected of an idealized area distribution. There are a few examples, however, of wind-tunnel models that have evidenced a very low drag rise. The wings of these configurations were also twisted and cambered in order to minimize the drag at lift. Thus, these configurations have yielded about the highest lift-drag ratio thus far obtained at transonic and supersonic speeds. The maximum lift-drag ratios $(L/D)_{MAX}$ are shown in figure 12. Of special interest is the wing-body combination designed for $M = 1.4$ (ref. 2) that uses a wing with a streamwise root thickness of 12 percent chord. This design was made possible by careful contouring of the wing-body juncture according to supersonic area-rule concepts. Up to $M = 1.4$, the characteristics of this wing compare very favorably with the 63° swept wing of thinner and more flexible construction that was designed for $M = 1.53$ (ref. 7). Details of the 68° swept wing designed for $M = 1.6$ can be found in reference 8. Figure 12 also illustrates the well-known fact that the values of $(L/D)_{MAX}$ obtainable at supersonic speeds - at least by conventional means - are low compared with subsonic values.

CURRENT RESEARCH TRENDS

The possibility of obtaining more complete cancellation of wave drag for wing-body combinations operating at supersonic speeds is being explored analytically and experimentally by the NACA. Some recent theoretical work of Heaslet and Lomax of the Ames Laboratory is of interest. Briefly, they are exploring the effectiveness of distorting the cross-sectional shape in varying degrees along the body length according to a calculated pattern in order to achieve a more substantial reduction in drag. The NACA is continuing experimental work of a similar nature on the effects of asymmetric wing-body modifications under lifting conditions. Important research on the interference effects of jets on drag is under way. The problem of handling inlet air and assessing its effect on the drag is also being actively pursued. New methods of analysis are being explored. Most of these developments in general have not reached a stage where concrete recommendations regarding their use can be made and are mentioned here only to emphasize the fact that this is a rapidly changing field of research, in which many people are working and new contributions may be expected.

[redacted]

CONCLUSIONS

At the present time, there are certain conclusions that can be drawn relative to the work done thus far on the problem of reducing wave drag, as follows:

1. The area rule is a powerful tool that provides guidance for the airplane designer in selecting aerodynamic features compatible with low wave drag.

2. Analytical methods have been developed that permit quantitative evaluation of the wave-drag level likely to be experienced with a given design.

3. For any airplane configuration, a high effective fineness ratio and smooth area progressions along the equivalent body for the design Mach number are essential to achieving a low wave-drag level.

4. Continued research is needed especially to exploit the possibilities of more complete cancellation of wave drag and regarding the effects of jet inlet and exit flows on airplane drag.

Langley Aeronautical Laboratory,
National Advisory Committee for Aeronautics,
Langley Field, Va., June 8, 1954.

[redacted]

REFERENCES

1. Whitcomb, Richard T.: A Study of the Zero-Lift Drag-Rise Characteristics of Wing-Body Combinations Near the Speed of Sound. NACA RM L52H08, 1952.

2. Whitcomb, Richard T., and Fischetti, Thomas L.: Development of a Supersonic Area Rule and an Application to the Design of a Wing-Body Combination Having High Lift-to-Drag Ratios. NACA RM L53H31a, 1953.

3. Jones, Robert T.: Theory of Wing-Body Drag at Supersonic Speeds. NACA RM A53H18a, 1953.

4. Whitcomb, Richard T.: Recent Results Pertaining to the Application of the "Area Rule." NACA RM L53I15a, 1953.

5. Holdaway, George B.: Comparison of Theoretical and Experimental Zero-Lift Drag-Rise Characteristics of Wing-Body-Tail Combinations Near the Speed of Sound. NACA RM A53H17, 1953.

6. Nelson, Robert L., and Stoney, William E., Jr.: Pressure Drag of Bodies at Mach Numbers Up to 2.0. NACA RM L53I22c, 1953.

7. Olson, Robert N., and Mead, Merrill H.: Aerodynamic Study of a Wing-Fuselage Combination Employing Wing Swept Back 63°. - Effectiveness of an Elevon as a Longitudinal Control and the Effects of Camber and Twist on the Maximum Lift-Drag Ratio at Supersonic Speeds. NACA RM A50A31a, 1950.

8. Brown, Clinton E., and Hargrave, L. K.: Investigation of Minimum Drag and Maximum Lift-Drag Ratios of Several Wing-Body Combinations Including a Cambered Triangular Wing at Low Reynolds Number and at Supersonic Speeds. NACA RM L51E11, 1951.

[redacted]

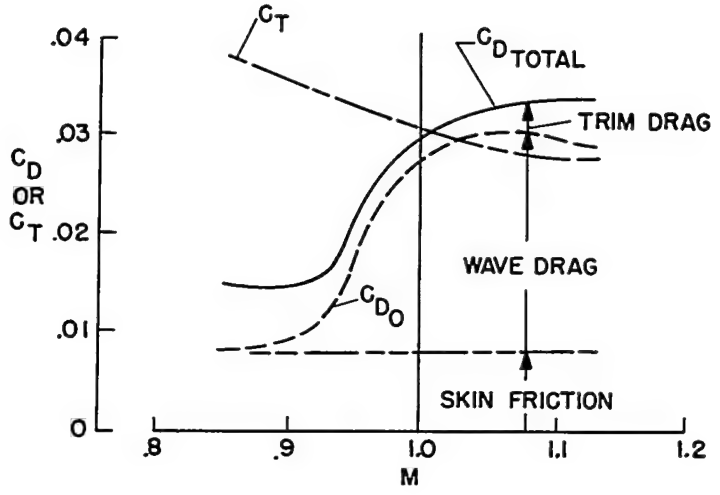

Figure 1.- Composition of drag for delta-wing design in level flight at an altitude of 35,000 feet.

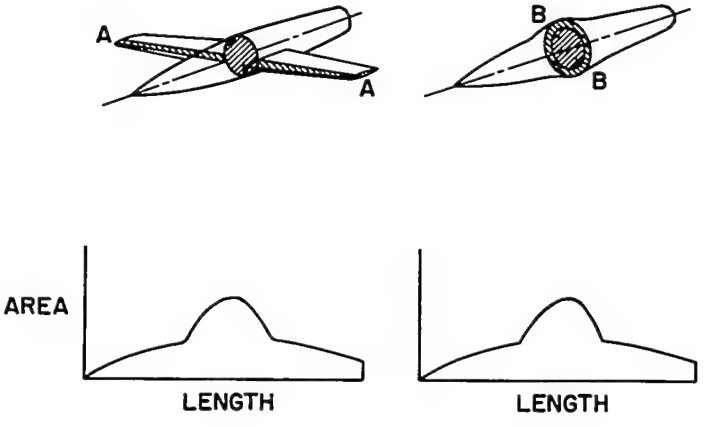

Figure 2.- Wing-body combination and equivalent body.

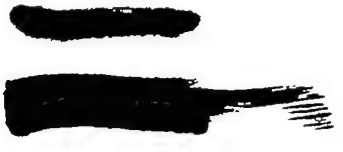

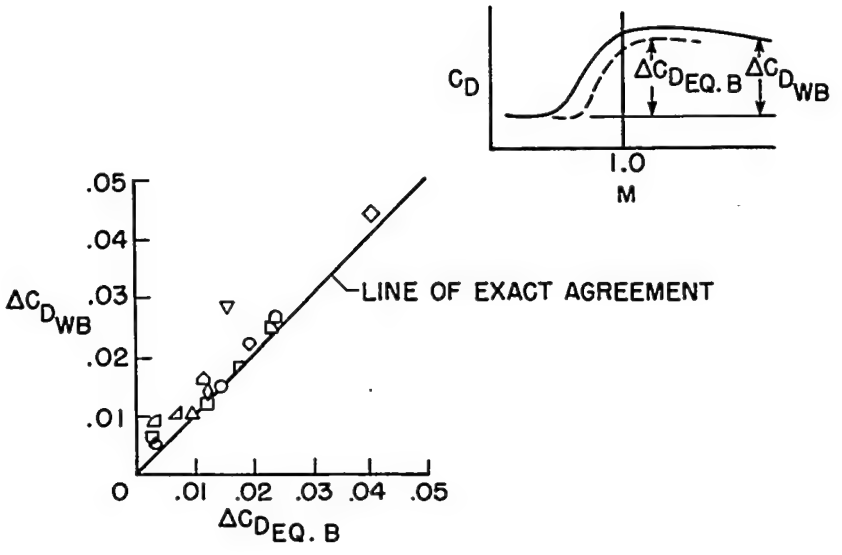

Figure 3.- Comparison of experimental drag-rise coefficients at M = 1.03.

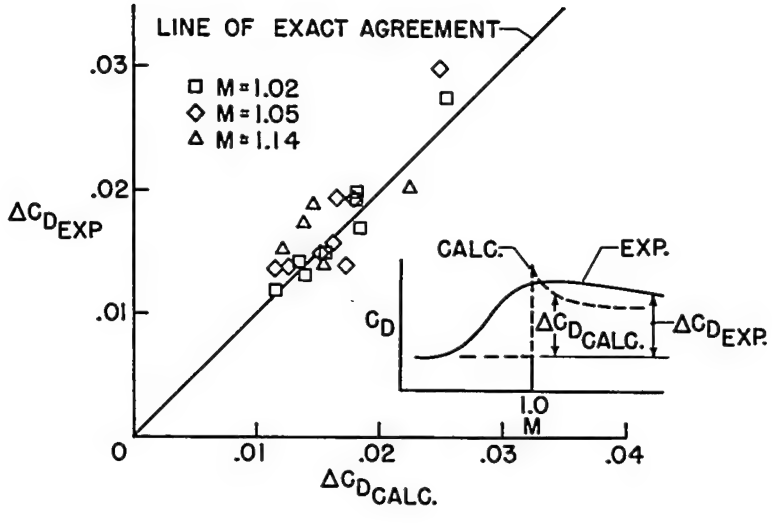

Figure 4.- Comparison of calculated and experimental drag-rise coefficients.

[redacted]

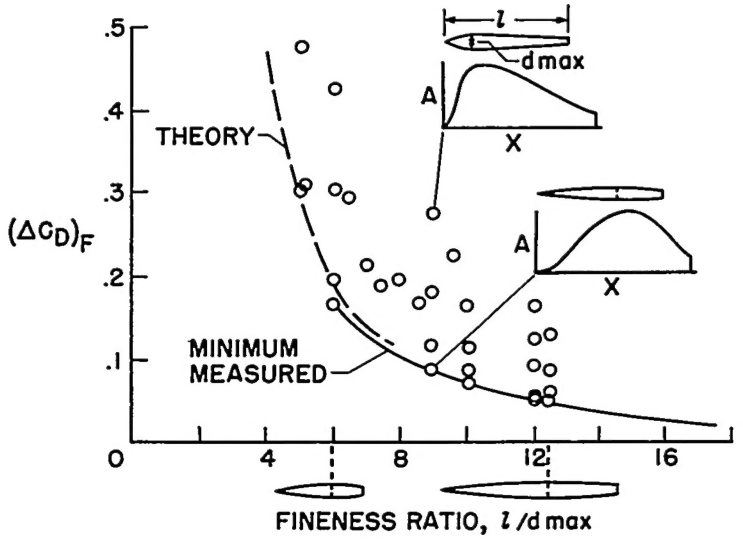

Figure 5.- Effects of fineness ratio and profile shape on body drag.

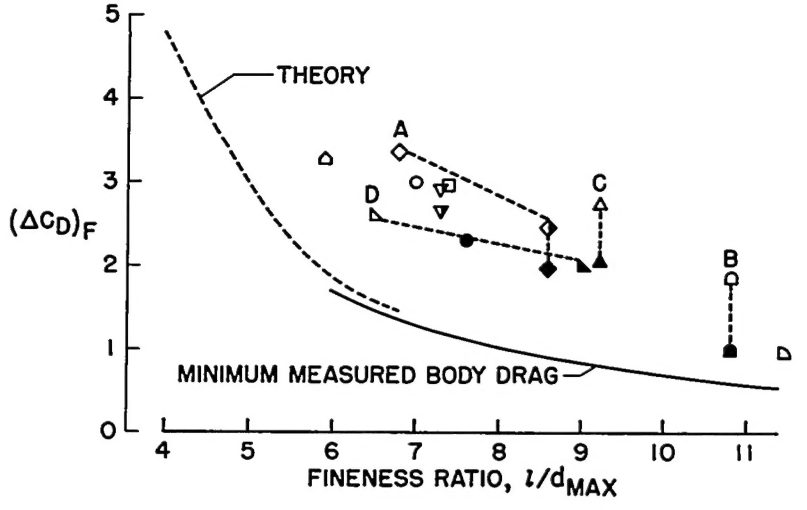

Figure 6.- Airplane drag rise based on fineness ratio and frontal area of equivalent body.

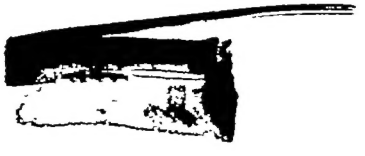

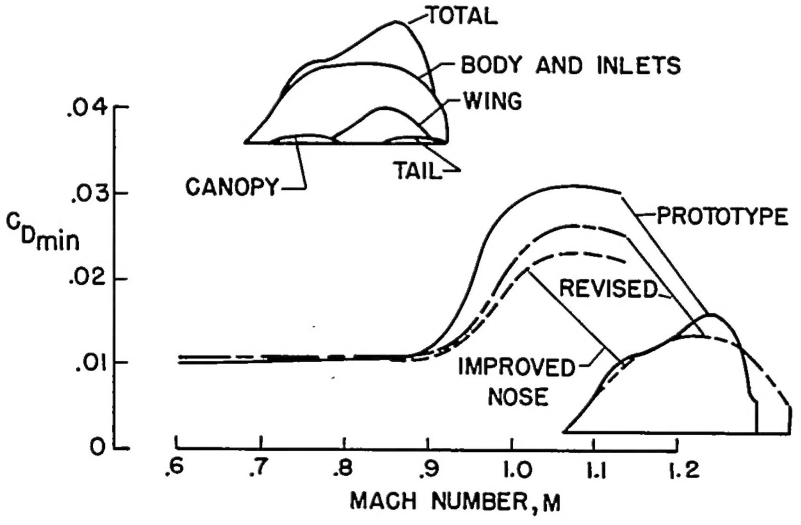

Figure 7.- Example A. Effect of body modifications on delta-wing airplane.

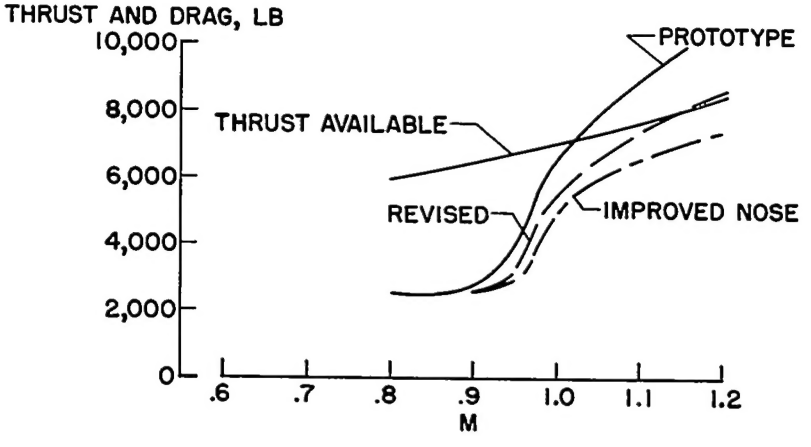

Figure 8.- Effect of body modification on performance of delta-wing airplane at 35,000 feet.

[redacted]

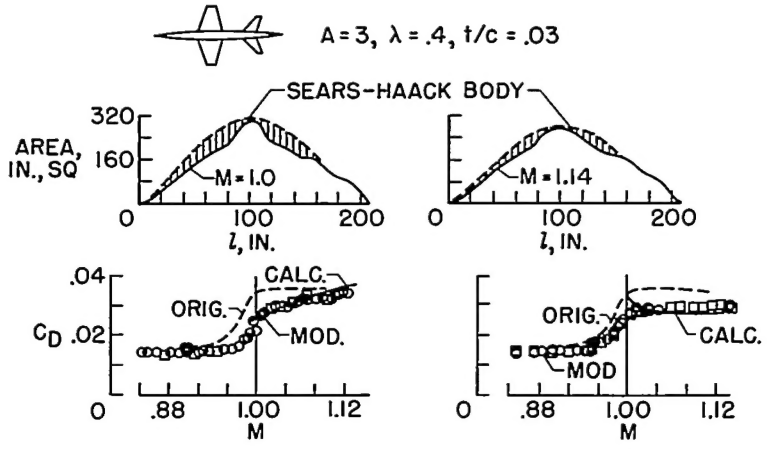

Figure 9.- Example B. Effect of adding volume to unswept-wing airplane.

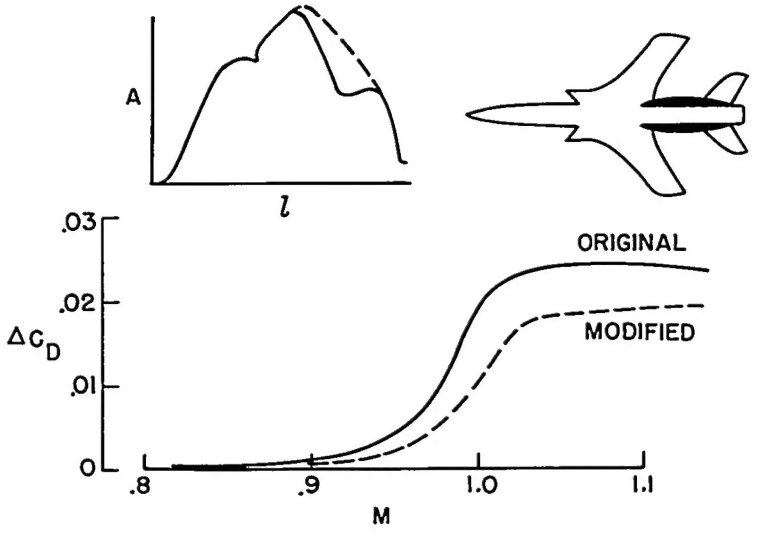

Figure 10.- Example C. Effect of adding volume to swept-wing airplane.

[redacted]

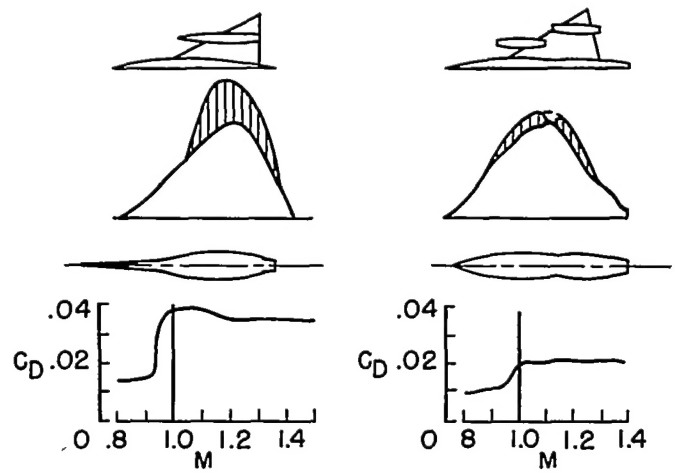

Figure 11.- Example D. Applications of area-rule concepts to multiengine airplane.

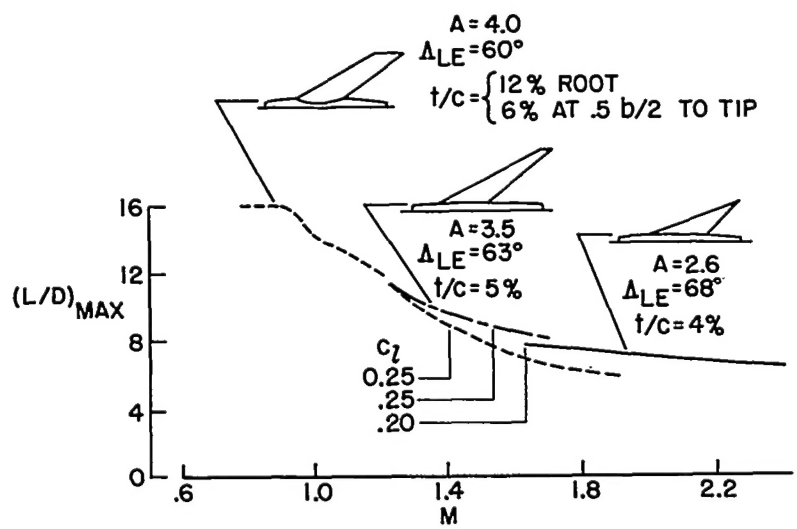

Figure 12.- High $\left(\frac{L}{D}\right)_{MAX}$ configurations.